



Removal of aqueous metazachlor, tembotrione, tritosulfuron and ethofumesate by heterogeneous monopersulfate decomposition on lanthanum-cobalt perovskites



Rafael R. Solís ^{a,b,*}, F. Javier Rivas ^{a,b}, Olga Gimeno ^{a,b}

^a Department of Chemical Engineering and Physical Chemistry, University of Extremadura, Av. Elvas s/n, 06006 Badajoz, Spain

^b University Institute of Water Research, Climate Change and Sustainability, IACYS, University of Extremadura, Av. Elvas s/n, 06006 Badajoz, Spain

ARTICLE INFO

Article history:

Received 22 April 2016

Received in revised form 16 June 2016

Accepted 23 June 2016

Available online 24 June 2016

Keywords:

LaCoO₃ perovskite

Oxone

Monopersulfate

Herbicides

Oxidation

ABSTRACT

This study reports LaCoO₃ perovskite oxide activity in the removal of aqueous herbicides (metazachlor, tembotrione, tritosulfuron and ethofumesate) by means of potassium monopersulfate (MPS) decomposition. The influence of initial MPS concentration and catalyst load have been assessed. MPS is instantaneously absorbed onto the perovskite surface where this species decomposes. Thus, MPS breakage leads to the formation of powerful oxidizing radicals which react with herbicides in solution. Tritosulfuron was the most recalcitrant compound towards this technology. Catalyst stability was tested by means of consecutive reuse cycles. No appreciable loss of activity was experienced. Experiments in the presence of *tert*-butyl alcohol, methanol and carbonate outlined the importance of radicals in herbicides degradation. Finally, synthesized LaCoO₃ was characterized. Scanning and transmission electron microscopy showed the presence of nanosized material, mostly spherical shaped, with 15.20 m² g⁻¹ of BET area. LaCoO₃ perovskite structure was corroborated by diverse techniques such as X-ray fluorescence (La:Co atomic ratio of 1:1), X-ray photoelectron spectroscopy (surface Co(III) and La(III)), and X-ray diffraction (rhombohedral LaCoO₃ phase).

© 2016 Elsevier B.V. All rights reserved.

1. Introduction

Farming uses large amounts of herbicides which usually run off into water resources. Therefore, a large list of different herbicides and pesticides is frequently detected in surface waters as micropollutants [1,2]. These discharges suppose a great environmental impact causing undesirable effects on non-targeted species.

Metazachlor (C₁₄H₁₆ClN₃O, CAS 67129-08-2, METAZ) belongs to chloroacetamide family, tembotrione (C₁₇H₁₆ClF₃O₆S, CAS 335104-84-2, TEMB) is a synthetic β -triketone, tritosulfuron (C₁₃H₉F₆N₅O₄S, CAS 142469-14-5, TRITO) is a sulfonylurea and ethofumesate (C₁₃H₁₈O₅S, CAS 26225-79-6, ETHO) is an example of benzofuran selective systemic herbicide. All of them are commonly applied as pre and post-emergence control of diverse weeds in a wide variety of crops. Table S1 shows some of their most important properties. Although the majority of these herbicides are relatively new in use, their occurrence in water is being screened at ng L⁻¹ or even μ g L⁻¹ levels [1–5].

Oxone® (2KHSO₅·KHSO₄·K₂SO₄) is the commercial name of the main source of potassium monopersulfate (MPS), which is considered a versatile and environmentally friendly oxidant used for bleaching, cleaning and disinfection. MPS is attracting attention due to its capacity of producing sulfate radicals which have some advantages over hydroxyl radical, such as higher oxidation potential, higher selectivity and effectiveness, wider pH range for reaction and higher half-life [6].

MPS can be activated by means of temperature [7], UV radiation [8], and metallic catalysts [7]. Hence, cobalt is catalogued as one of the best transition metal in the homogeneous activation of MPS [9]. However, homogeneous catalysis requires the further removal of the catalyst, especially in those cases where the active substance presents toxic properties. Actually, cobalt shows toxicity and causes health problems at very low concentrations, leading to the development of asthma, pneumonia and cardiomyopathy [10]. As a consequence, developing heterogeneous catalysts containing cobalt for MPS activation seems to be a challenging and promising alternative. Nevertheless, acid conditions usually lead to cobalt leaching. Thus, this latter aspect has to be taken into account.

A number of previous studies have investigated the heterogeneous catalytic decomposition of MPS using cobalt oxides such

* Corresponding author.

E-mail address: rrodrig@unex.es (R. R. Solís).

as CoO and Co_3O_4 [11], spinel cobalt ferrite (CoFe_2O_3) [12], and cobalt supported onto diverse materials like different oxides (TiO_2 , MgO , Al_2O_3 , SiO_2 , MnO_2 or ZnO) or activated carbon [6]. In a high number of cases, problems associated to cobalt leaching have been experienced.

Perovskite oxides derive from the ABO_3 structure, where the A cation is larger than the B cation. LaXO_3 perovskite oxides have been demonstrated to be active in wet peroxide oxidation processes [13]. Lanthanum perovskites have successfully been used in catalytic ozonation [14] and some H_2O_2 and/or UV mediated processes [15]. Nevertheless, to author's knowledge, no attention to LaCoO_3 as a MPS activator has been paid.

The present study reports the use of LaCoO_3 perovskite oxide in MPS activation. LaCoO_3 has been synthesized, and the solid characterized by means of nitrogen isotherm adsorption, scanning and transmission electron microscopy, X-ray photoelectron spectroscopy, X-ray fluorescence and X-ray diffraction. LaCoO_3 and MPS combination has been applied to a mixture of four herbicides in water (metazachlor, tembotrione, tritosulfuron and ethofumesate). The effectiveness of LaCoO_3 and MPS combination has been studied varying MPS concentration, catalyst load and solution pH, which are the main operating variables. Cobalt leaching has also been considered at different operating pHs. Catalyst reusability and radical scavenger presence have also been assessed.

2. Experimental

2.1. Materials

Analytical herbicide Pestanal® standards were purchased from Sigma-Aldrich®. Oxone® was acquired from Sigma-Aldrich®. Lanthanum(III) nitrate hexahydrate (>99.99%) from Aldrich®, cobalt(II) acetate tetrahydrate (>98%) from Sigma-Aldrich® and citric acid (99%) from Aldrich® were used for perovskite synthesis. The rest of chemicals were purchased from Sigma-Aldrich and used as received.

Acetonitrile from VWR Chemicals was used in HPLC determination of herbicides in water. All solutions were prepared with ultrapure water from a Mili-Q® academic (Millipore) system (18.2 $\text{M}\Omega \text{ cm}$).

2.2. Catalyst synthesis and characterization

LaCoO_3 perovskite was synthesized in the presence of citric acid as complexing organic agent [16]. In a typical synthesis run, $\text{La}(\text{NO}_3)_3 \cdot 6\text{H}_2\text{O}$ and $\text{Co}(\text{CH}_3\text{COO})_2 \cdot 4\text{H}_2\text{O}$ with a molar ratio $\text{La:Co} = 1:1$ were dissolved in 400 mL of ultrapure water. After 1 h mixing under magnetic agitation, 100 mL of citric acid in excess (twice the stoichiometrically needed for each metal [16]) was slowly added. The resultant solution was heated at 100 °C to remove water excess, drying thereafter the obtained pinkish gel. The solid was grinded and calcined at 700 °C for 7 h. This catalyst was used in all experiments.

pH of point of zero charge (pH_{pzc}) was obtained by mass titration method [17]. Briefly, a solution of HNO_3 0.1 M was prepared and pH adjusted until value of 3 with NaOH 0.1 M. Different containers with increasing amounts of solid (0.05, 0.1, 0.5, 1, 5, 10 and 20%) were filled with 15 mL of solution. Solutions were kept under stirring and pH was measured after 48 h of equilibria. A plot of pH versus solid fraction (%) gives a curve which tends asymptotically to pH_{pzc} value.

BET surface area was quantified by means of nitrogen adsorption isotherms obtained at 77 K with a Quadasorb instrument (Quantachrome). Prior to analysis, samples were treated at 150 °C for 24 h under high vacuum conditions.

Scanning electron microscopy (SEM) was conducted in a Hitachi-S-4800 coupled to a secondary electrons detector (acceleration voltage 20 kV) while transmission electron microscopy (TEM) analysis was applied using a TEM Tecnai G2 20 Twin-FEI company apparatus (filament LaB_6 , voltage 200 kV, magnification up to 1.05 10^6).

X-ray photoelectron spectroscopy (XPS) spectra were obtained using a XPS K-alpha-Thermo Scientific device, working with a $\text{K}\alpha$ monochromatic source of Al (1486.68 eV). A value of 284.8 eV for the C 1s peak was taken to calibrate the signals of the rest peaks. High resolution of XPS spectra for La 3d, Co 2p and O 1s were recorded.

The XRF measurements were carried out by a sequential wavelength dispersive X-ray Fluorescence (WDXRF) spectrometer (S8 Tigger, Brucker) equipped with an X-ray tube of rhodium anode operating at 60 kV, and 170 mA.

Thermal Gravimetry, Differential Temperature Analysis and released gases Mass Spectrometry (TG-DTA-MS) was performed with a Setaram SETSYS Evolution-16 equipment connected to a PrismaTM QMS200 quadrupole mass spectrometer. The operation conditions were: sample loading 21 mg, air flow rate 50 mL min^{-1} and heating rate of 10 °C min^{-1} from room temperature to 800 °C.

Crystalline phases were analyzed by X-ray diffraction (XRD), in a Bruker D8 Advance diffract meter equipped with a monochromator of Ge 111 $\text{K}\alpha$ of Cu (wavelength, 1.5456 Å). A temperature chamber complemented the installation in order to obtain diffractograms through temperature.

2.3. Experimental setup and procedure

The experimental reaction system basically consisted of a 1.0 L borosilicate cylindrical glass vessel. It was magnetically stirred by an IKA® RCT stirrer equipped with temperature control. The reactor was filled with 1.0 L of herbicides (1 mg L^{-1} of each) water solution. pH was adjusted by NaOH addition (10 or 1 M). In order to start the reaction, a small volume (less than 10 mL) of a high concentrated MPS solution was initially added, and pH was thereafter readjusted. Previously, to achieve the adsorption equilibrium, the solution was kept under stirring for 30 min. Samples were regularly extracted at different times and filtered with Millex-HA filters (Millipore, 0.45 μm). HPLC samples were quenched with $\text{Na}_2\text{S}_2\text{O}_3$ 0.5 M (10 μL per 1 mL of sample).

2.4. Analytical methods

Herbicides were analyzed by an Agilent 1100 (Hewlett-Packard) High Performance Liquid Chromatography equipped with UV detection (HPLC-UV). The column used was a Kromasil 100 5C18 (5 μm , 2.1 \times 150 mm). A mobile phase composed by 0.1% H_3PO_4 acidified water (A) and acetonitrile (B) was pumped at a flow rate of 1 mL min^{-1} , with an isocratic percentage composition of 55:45 A:B. UV detection was conducted at 220 nm. Observed retention times were 6.4, 11.3, 12.5 and 14.9 min for metazachlor, tembotrione, tritosulfuron, and ethofumesate, respectively. Fig. S1 shows a typical example of chromatogram.

MPS concentration evolution was analyzed spectrophotometrically by a colorimetric method based on *N,N*-diethyl-*p*-phenylenediamine (DPD) oxidation [18].

Cobalt leaching was quantified by means of atomic absorption, using a Varian SpectrAA Series 140 instrument. Alternatively, this cation was also analyzed spectrophotometrically by the zincon method [19].

pH of the reaction media was monitored, adjusted and controlled by means of a Crison GLP 21+ pH meter, whose electrode was submerged into the reactor.

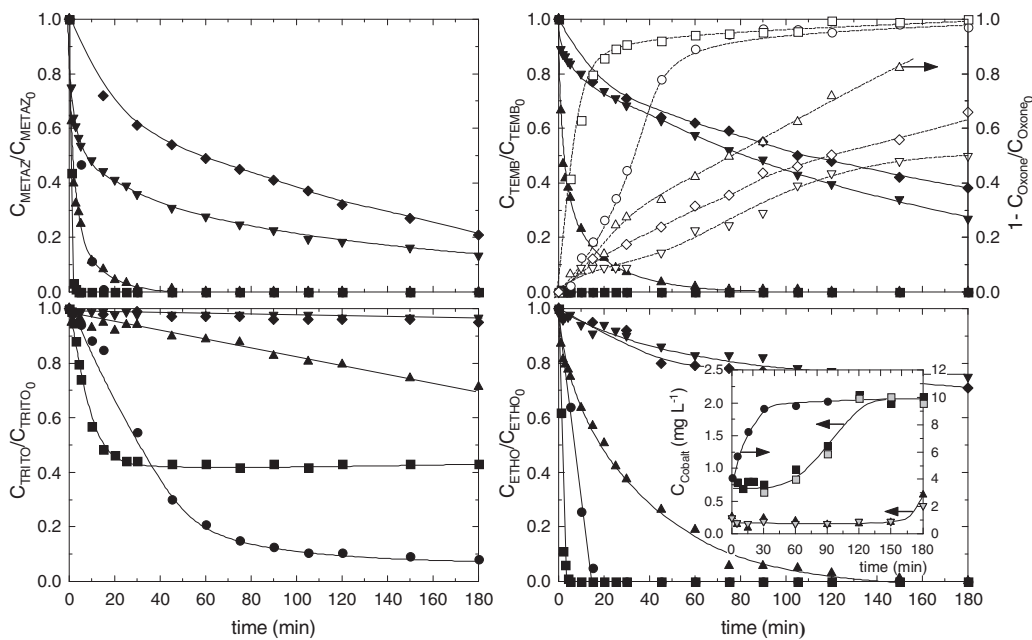


Fig. 1. Oxone® mediated elimination of a mixture of herbicides in the presence of LaCoO₃. Influence of pH. Experimental conditions: $C_{\text{Herbicide}} = 1 \text{ mg L}^{-1}$ each, $C_{\text{LaCoO}_3} = 0.5 \text{ g L}^{-1}$, $T = 20^\circ\text{C}$, $C_{\text{Oxone}_0} = 1.0 \cdot 10^{-4} \text{ M}$, pH: ●, 3.0; ■, 5.0; ▲, 7.0; ▼, 9.0; ♦, 7.0, homogeneous contribution. Open symbols in top right figure: Oxone® conversion. Inset figure: leached cobalt (grey filled symbols correspond to atomic absorption analysis, black ones were spectrophotometrically obtained).

3. Results and discussion

3.1. Operating variables influence

3.1.1. pH influence and cobalt leaching

As stated in the introduction section, one of the main drawbacks in using heterogeneous catalysts containing transition metals is the deactivation of the catalyst due to leaching of these metals into the water bulk [20]. Additionally, homogeneous catalysis of dissolved metals may mislead to the interpretation of the results obtained. Accordingly, a first experimental series was conducted at different pH operating conditions. In addition to parent compound removal, leached cobalt was also monitored in these experiments.

Fig. 1 shows the results obtained when pH 3, 5, 7, and 9 were used. Previous to these experiments, blank runs demonstrated the negligible reactivity of monopersulfate alone towards individual herbicides (the exception was tembotrione). However, some conversion was obtained in all herbicides when treated with MPS simultaneously (likely, tembotrione partial conversion generates some species capable of reacting with the rest of herbicides).

As observed in Fig. 1, the system is more effective at low pH. Hence, instantaneous 100% conversion (less than 1 min) of metazachlor, tembotrione and ethofumesate was experienced when pH values in the range 3–5 were used. Tritosulfuron was the most recalcitrant compound, requiring more than 100 min to achieve 90% elimination. Inset in Fig. 1 depicts the evolution of cobalt in water. At the sight of the figure, a significant leaching of cobalt to water bulk was obtained when the working pH was 3. The concentration of this transition metal was as high as 4 mg L^{-1} even before the addition of Oxone®, (leached during the 30 min adsorption period). Under these conditions, the homogeneous reaction predominates over the heterogeneous path. Moreover, as the reaction progresses, the concentration of cobalt reaches values in the proximity of 10 mg L^{-1} . Oxone® is easily decomposed in the presence of dissolved cobalt leading to radical species [11]. Hence, monopersulfate concentration rapidly decreases at pH 3 and 5. As a consequence, tritosulfuron abatement comes to a halt when Oxone® conversion reaches roughly 90%. Homogeneous catalyzed

Oxone® decomposition rate is favored at alkaline conditions [21], explaining why the peroxide is faster removed at pH 5 than at pH 3, even when cobalt concentration is lower at the more basic pH. Monopersulfate decomposition orders regarding Co^{2+} and H^+ concentrations are 1 and –1, respectively [22]. Accordingly, a 5–10 fold increase in dissolved cobalt concentration exerts a lower influence than a 100-fold decrease in protons. At circumneutral or basic pH, leached cobalt concentration is quite low (below 0.2 mg L^{-1} or $3.4 \cdot 10^{-6} \text{ M}$). The homogeneous contribution was analyzed at neutral pH by carrying out an experiment in the presence of 0.2 mg L^{-1} of cobalt, which is the observed cobalt lixiviated at this pH. The results revealed that herbicide conversions were similar to those obtained in a blank run in the presence of Oxone® and absence of cobalt and catalyst.

pH reduces cobalt leaching and decreases monopersulfate abatement. The pH_{pzc} value of the catalyst was found to be 9.08 (Fig. S2). This explains the ability of the catalyst to adsorb anions, such as monopersulfate, at acidic or neutral pH since its surface is positively charged. The low MPS decomposition at pH = 9 is likely related to its second acid dissociation $\text{pK}_a = 9.4$.

3.1.2. Oxone concentration

Taking into account the results obtained in the previous section, in order to avoid cobalt leaching and limit this study to the heterogeneous catalysis, next experiments were conducted at pH 7, a compromise between leached cobalt and reaction rate.

The influence of the initial Oxone® concentration was studied in the range 10^{-4} – 10^{-3} M . Fig. 2 shows the results obtained in this experimental series. As inferred from this figure, Oxone® concentrations above $5 \cdot 10^{-4} \text{ M}$ led to the instantaneous removal of metazachlor, tembotrione and ethofumesate while tritosulfuron required almost one hour to completely disappear when $5 \cdot 10^{-4} \text{ M}$ in Oxone® was used. As stated previously, experiments in the absence of perovskite did show some reactivity of Oxone® towards the herbicides when simultaneously treated.

An analysis of Oxone® uptake (measured as moles of monopersulfate consumed per mol of herbicide abated, see Fig. 3), applied to the two runs conducted with the lowest oxidant

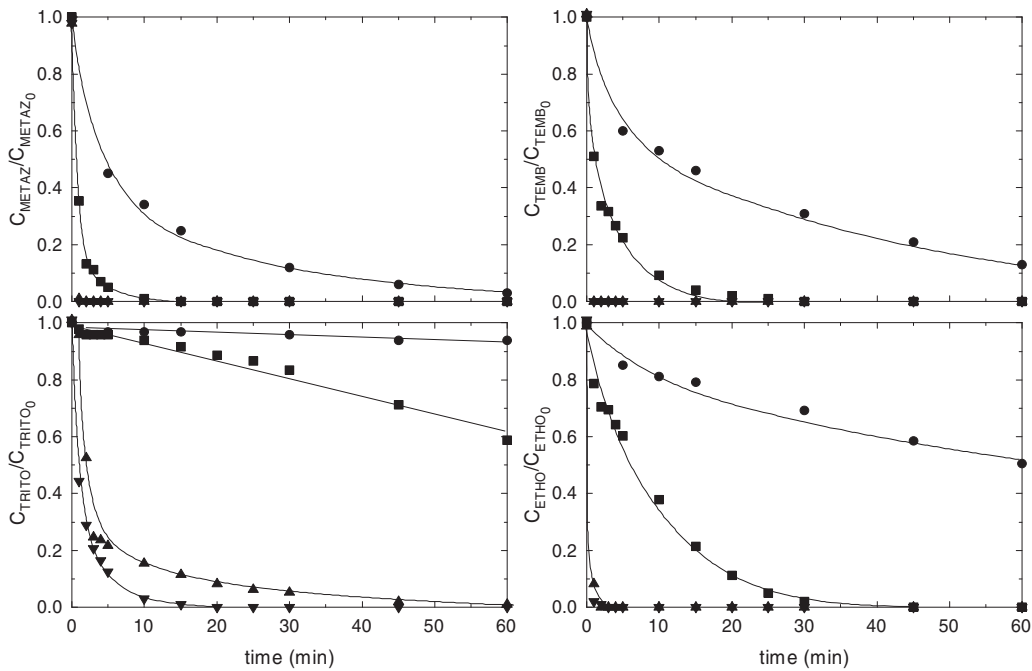


Fig. 2. Oxone® mediated elimination of a mixture of herbicides in the presence of LaCoO₃. Influence of initial Oxone® concentration. Experimental conditions: C_{Herbicide} = 1 mg L⁻¹ each, pH = 7, C_{LaCoO₃} = 0.5 g L⁻¹, T = 20 °C. C_{Oxone,0} · 10⁴(M): ●, 1.0; ■, 2.0; ▲, 5.0; ▼, 10.

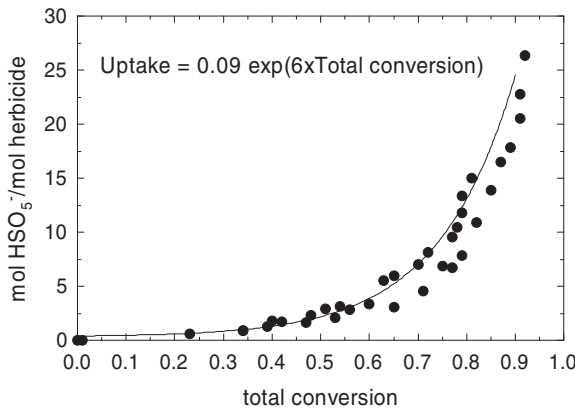


Fig. 3. Oxone® mediated elimination of a mixture of herbicides in the presence of LaCoO₃. Monopersulfate uptake as a function of total conversion. Experimental conditions: C_{Herbicide} = 1 mg L⁻¹ each, pH = 7, C_{LaCoO₃} = 0.5 g L⁻¹, T = 20 °C. C_{Oxone,0} = 1.0–2.0 · 10⁻⁴ M.

concentration revealed an efficient consumption of the oxidant up to values of 60–70% of total herbicides conversion; thereafter, the stoichiometric coefficient sharply increased by following an exponential growth, likely due to the accumulation of intermediates competing for the active oxidizing species generated.

From a practical point of view, conversion values below 70% are recommended provided that the effluent can be further polished in a biological step or fulfill the regulatory laws of direct discharge. At this point, it should be pointed out that 70% total conversion involves the complete elimination of metazachlor and tembotriione and 80% removal of ethofumesate. Tritosulfuron, being the most recalcitrant compound only achieves a scarce 10% oxidation.

3.1.3. Catalyst concentration influence

An additional experimental series was conducted at different perovskite concentrations by maintaining the rest of operating variables constant. Fig. 4 depicts the results obtained when 10⁻⁴ M in Oxone® was used.

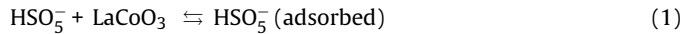
As a rule of thumb, perovskite amount exerts a positive influence on herbicides conversion, although global differences are minor when analyzing the results of total herbicide abatement achieved when 0.5, 1.0 and 1.5 g L⁻¹ of catalyst were used (see bottom-right inset of Fig. 4 which depicts total conversion versus time).

Once more, Fig. 4 confirms the recalcitrance of tritosulfuron if compared to the reactivity of the rest of herbicides. The shape of the curves revealed a fast initial period (first 2–3 min) where herbicide concentration sharply decreases. Thereafter, the removal rate slows down resembling first order like kinetics. A priori, this behavior cannot be attributed to a fast adsorption of herbicides. Hence, previous to each experiment, the herbicides solution is stirred in the presence of perovskite for 30 min with negligible change in their aqueous concentration.

On the one hand, the rise of catalyst load does significantly affect the rate of decomposition of monopersulfate (top-left inset of Fig. 4) which denotes the role played by the catalyst in the formation of radicals. On the other hand, a high amount of solid seems to negatively affect the monopersulfate efficient uptake (top-right inset of Fig. 4). Hence, a slightly higher consumption of Oxone® was experienced when 1.5 g L⁻¹ of LaCoO₃ was used, not leading to an appreciable improvement in herbicides total conversion if compared to results obtained when lower solid concentrations were used.

Additionally, the bottom-left inset of Fig. 4 shows that the amount of cobalt leached was negligible, below 0.2 mg L⁻¹, and constant regardless of the initial perovskite concentration or elapsed reaction time. This small amount suggests a high stability of the catalyst which was thereafter checked by conducting some runs using the same recovered catalyst.

From the experimental results obtained previously the following simplified mechanism is proposed, taking monopersulfate and organic matter (represented as R) into account:



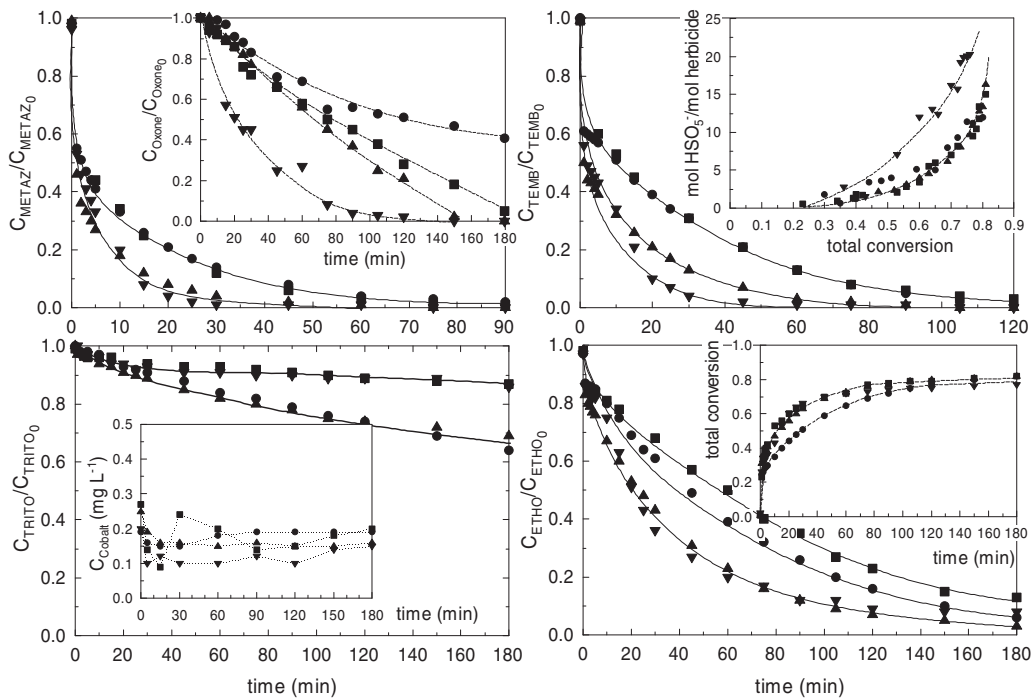


Fig. 4. Oxone® mediated elimination of a mixture of herbicides in the presence of LaCoO₃. Influence of perovskite concentration. Experimental conditions: C_{Herbicide} = 1 mg L⁻¹ each, pH = 7, T = 20 °C. C_{Oxone,0} = 1.0 10⁻⁴ M, C_{LaCoO₃} (g L⁻¹): ●, 0.25; ■, 0.50; ▲, 1.0; ▼, 1.5. Inset Figures: top-left, Oxone® normalized concentration; top-right, monopersulfate uptake; bottom-left, cobalt leached; bottom-right, total herbicide conversion.



Hence, the fast adsorption of monopersulfate until equilibrium would lead to the instantaneous generation of radicals and fast removal of herbicides. Thereafter, a chain radical mechanism would evolve accounting for the second slower stage. The second stage would be controlled by the rate of organic radical reactions.

3.1.4. Catalyst stability

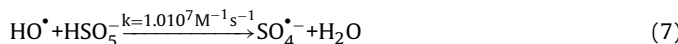
To ascertain the stability of the catalyst, six consecutive runs were conducted by recycling the catalyst used. As observed in Fig. 5, the solid maintains its activity even in the last run. This fact is also corroborated if considering the monopersulfate depletion profile shown in the embedded plot.

No appreciable cobalt leaching was experienced in these experiments.

3.1.5. Scavengers influence

The influence of radical scavengers was assessed by using *tert*-butyl alcohol (*t*-BuOH), Methanol (MeOH) and carbonates which react with hydroxyl and sulfate radicals with second order rate constants of 6 10⁸ M⁻¹ s⁻¹ [23] and 4 10⁵ M⁻¹ s⁻¹ [24], 9.7 10⁸ M⁻¹ s⁻¹ [25] and 3.2 10⁶ M⁻¹ s⁻¹ [26], and 8.5 10⁶ M⁻¹ s⁻¹ [27] and 9.1 10⁶ M⁻¹ s⁻¹ [28], respectively.

Fig. 6 reveals some interesting aspects. Hence, *tert*-butyl alcohol, a well-known hydroxyl radical scavenger, has no significant influence in the monopersulfate decomposition rate onto the perovskite surface. This fact suggests that monopersulfate is not decomposed by free hydroxyl radicals found in the solution bulk according to:



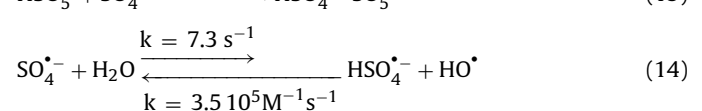
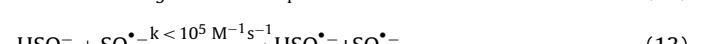
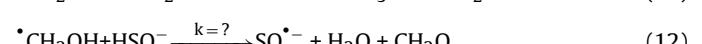
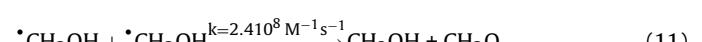
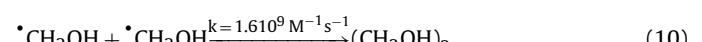
These results could be expected since herbicides compete with the promoter to trap the HO[•] species (Reaction (3)) showing

second order rate constants around 2–3 orders of magnitude higher. Accordingly, by considering the total herbicide concentration (roughly 12 μM) and an average second order rate constant of 5 10⁹ M⁻¹ s⁻¹, the ratio of the above competing reactions would be:

$$\text{Ratio} = \frac{k_{HO^\bullet, \text{herbicides}} C_{\text{herbicides}}}{k_{HO^\bullet, HSO_5^-} C_{HSO_5^-}} \approx \frac{5 10^9 \times 1.2 10^{-5}}{11 0^7 \times 2.0 10^{-5}} \approx 30 \quad (8)$$

However, the presence of the tertiary alcohol partially inhibits the removal rate of the herbicides, suggesting that HO[•] species are present in solution.

Given the particular effect of MeOH addition, this reaction was conducted by triplicate. The reproducibility of the results confirmed a fast inefficient monopersulfate depletion leading to a significant inhibition of herbicides removal. The inhibition is likely related to suppression not only of HO[•] but also of sulfate radicals due to their reactions with methanol. Additionally, monopersulfate would tentatively be decomposed by reacting with hydroxymethyl radicals (Eq. 12) initiating an inefficient chain mechanism in terms of herbicides removal. Additionally, the aforementioned hypothesis would sustain why tembotrione is less affected since this compound directly reacts with monopersulfate. The mechanism supporting these facts obeys the following reactions [22,28]:



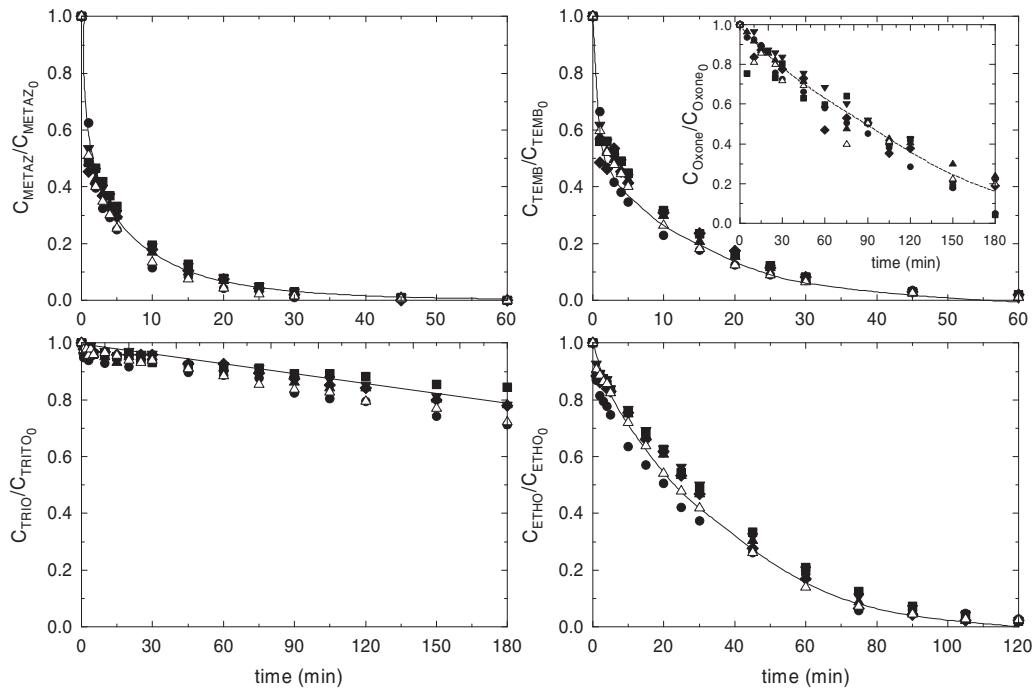


Fig. 5. Oxone® mediated elimination of a mixture of herbicides in the presence of LaCo₃. Influence of perovskite reuse. Experimental conditions: C_{Herbicide} = 1 mg L⁻¹ each, pH = 7, T = 20 °C. C_{Oxone,0} = 1.0 10⁻⁴ M, C_{LaCo3} = 0.5 g L⁻¹. ●, Fresh catalyst; ■, 1st reuse; ▲, 2nd reuse; ▼, 3rd reuse; ♦, 4th reuse, △, 5th reuse. Inset Figure: Oxone® normalized evolution.

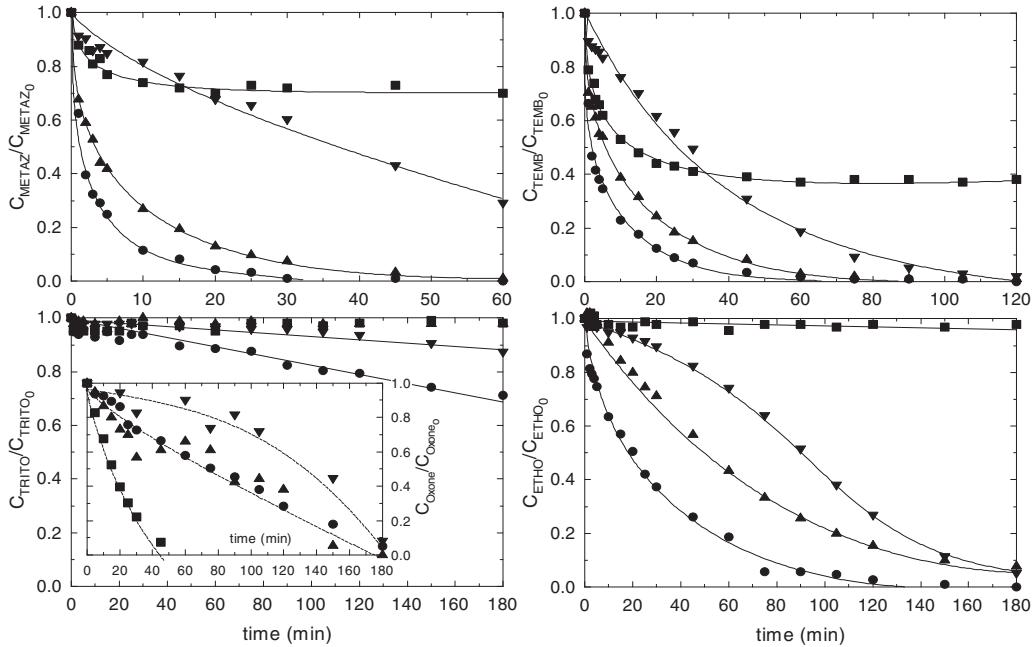
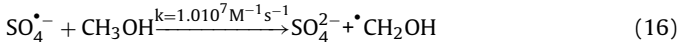


Fig. 6. Oxone® mediated elimination of a mixture of herbicides in the presence of LaCo₃. Influence of scavengers presence. Experimental conditions: C_{Herbicide} = 1 mg L⁻¹ each, pH = 7, T = 20 °C. C_{Oxone,0} = 1.0 10⁻⁴ M, C_{LaCo3} = 0.5 g L⁻¹, Scavenger: ●, No scavenger; ■, Methanol 10⁻² M; ▲, tert-Butanol 10⁻² M; ▼, Carbonates 5 10⁻³ M.



Carbonates negatively affect herbicides removal rates, likely due to radical scavenging. However, contrary to MeOH, monopersulfate is decomposed to a lower extent if compared to the experiments in the absence of scavengers. The explanation can be associated to two potential effects, on one hand by partially avoiding the

reactions of radicals and monopersulfate; and on the other hand, the most probable cause may be that carbonates could negatively affect the adsorption of Oxone® onto the perovskite surface impeding its decomposition.

3.2. Catalyst characterization

Fig. S3 reports results of nitrogen adsorption isotherm. As it could be observed, LaCo₃ provides a type II isotherm, which is

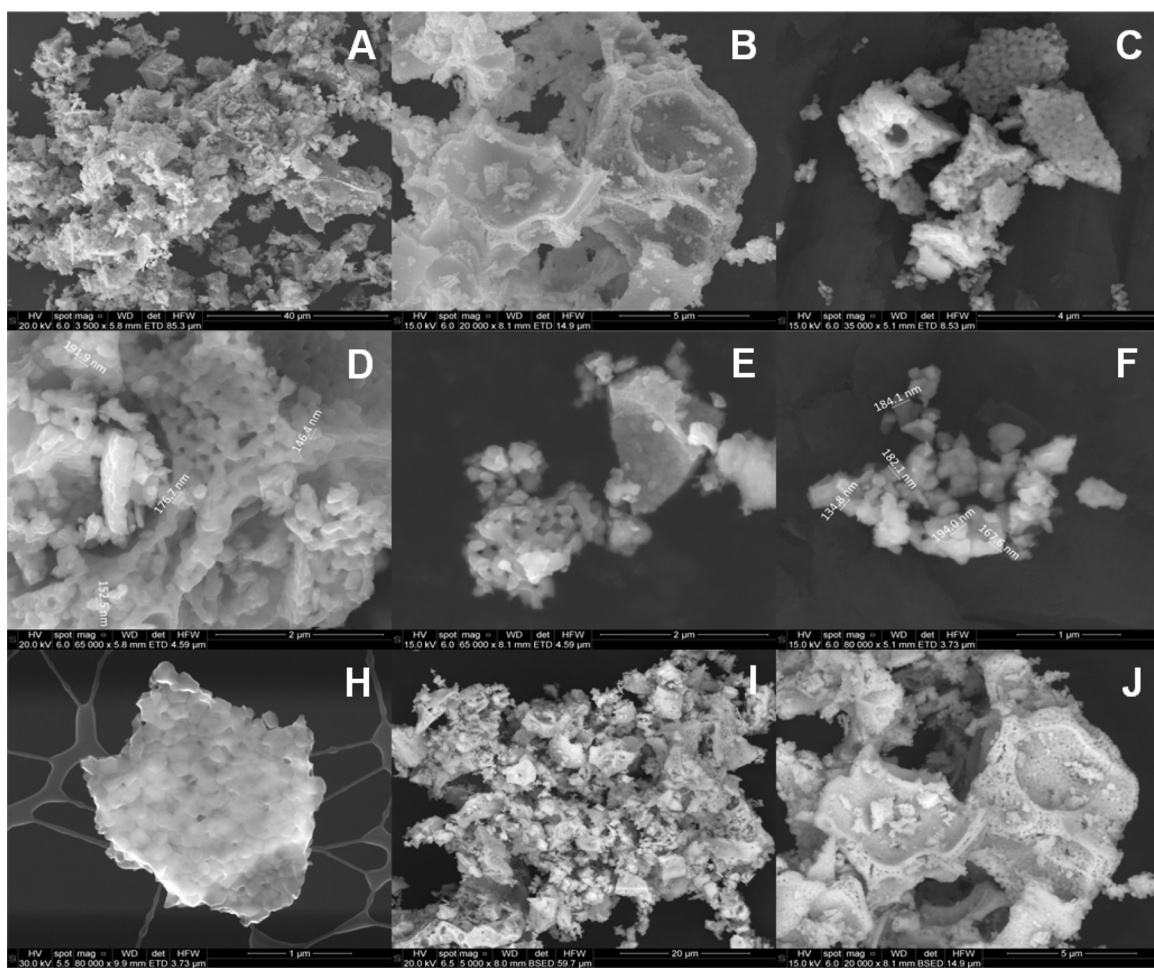


Fig. 7. LaCoO₃ powder SEM images obtained using secondary electrons (A–H) and backscattered electrons (I and J).

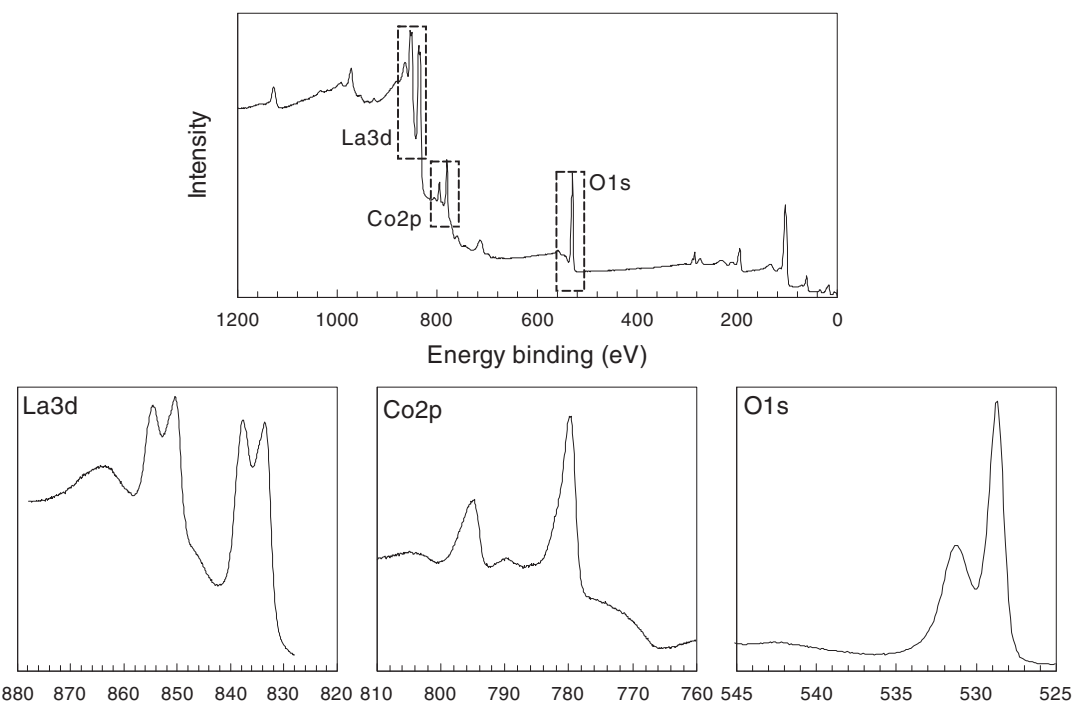


Fig. 8. XPS of LaCoO₃. General and high resolution spectra of La3d, Co2p and O1s.

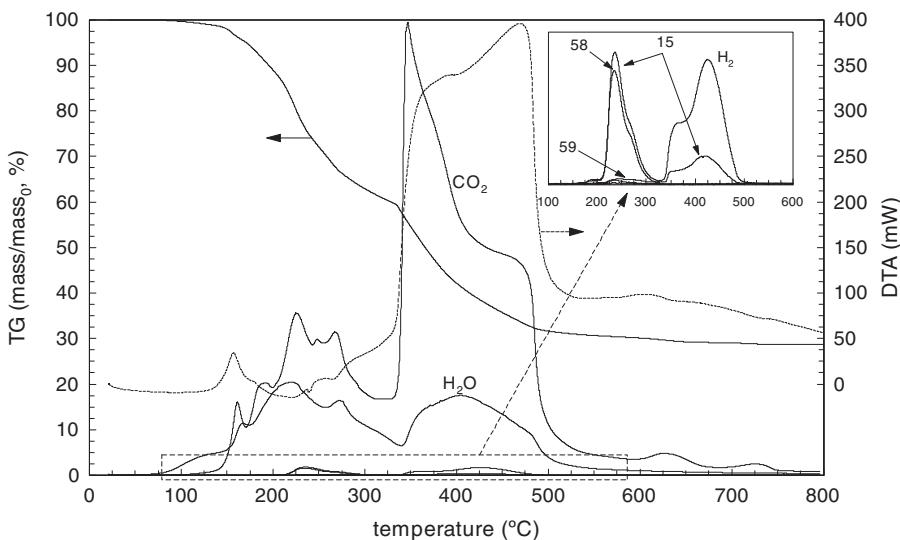


Fig. 9. TG-DTA-MS of uncalcined LaCoO_3 powder.

characteristic of non-porous or macroporous materials. In this kind of isotherm unrestricted monolayer and multilayer adsorption may take place. Multipoint BET surface area fitting (see Fig. S3 inset) in the range p/p_0 0.1–0.35 led to a specific surface area of $15.20 \text{ m}^2 \text{ g}^{-1}$, which is indicative of a non-porous material ($R=0.998$). It might proof the fact of a nanosized material. From this linear regression is also possible to obtain the C constant ($C=5.592$), which is related to the affinity and interaction of the solid with the adsorbate; and therefore, the heat of the process.

LaCoO_3 powder was also studied by means of Scanning Electron Microscopy (SEM). Diverse micrographs are summarized in Fig. 7. Firstly, main images, which are obtained from secondary electrons, verify the existence of homogeneous nanosized spherical particles, which are in the range 100–200 nm. This fact has been reported in literature [29,30]. However, these particles seem to form bigger agglomerates. Actually, some structures are made of these spherical particles, strongly linked to each other, where it is difficult to distinguish them. In others, the spherical aggregates are weakly linked. The biggest structures might have followed a pattern before grinding the powder in the synthesis process, as it could be discerned in some images. Secondly, from BackScattered Electrons (BSE) pictures (images I and J in Fig. 7), it is possible to analyze the homogeneity in terms of composition of the sample. Thus, the contrast in the image produced is determined by the distribution of different chemical phases in the sample. Accordingly, high homogeneity was observed, leading to the idea of one phase oxide composition. Thirdly, an Energy Dispersive X-ray (EDX, Fig. S4) analysis led to an elemental composition, expressed as atomic percentage, 22.12 ± 0.55 , 23.60 ± 1.31 , 54.28 ± 1.82 for La, Co and O, respectively.

Wavelength Dispersive X-ray Fluorescence (WDXRF) was also applied to calculate the proportion between cobalt and lanthanum (Fig. S5). Without taking oxygen into account, 49.45 ± 0.02 and $50.54 \pm 0.02\%$ of atomic La and Co was found, respectively (proportion La:Co = 1.00:1.02).

TEM analysis confirmed the morphology and size particle observed in SEM. Results are shown in Fig. S6. In this figure it is possible to observe that spherical particles illustrated in SEM micrographs are likely to be composed by smaller aggregates, whose size is inferior to 100 nm in some cases. Despite what is reported in others LaCoO_3 works [31,32], a clear crystal phase could not be confirmed from TEM analysis.

XPS technique was employed to analyze LaCoO_3 surface properties. Fig. 8 depicts general and high resolution spectra of $\text{La}3\text{d}$, $\text{Co}2\text{p}$ and $\text{O}1\text{s}$ regions. In $\text{Co}2\text{p}$ region two peaks can be appreciated, whose maximums are located at 794.8 and 779.9 eV. These values correspond to $\text{Co}2\text{p}_{1/2}$ and $\text{Co}2\text{p}_{3/2}$, respectively. $\text{Co}2\text{p}_{3/2}$ binding energy highly coincides with conventional value reported on Co_2O_3 and LaCoO_3 [33,34], were Co(III) state dominates. Furthermore, absence of satellite peaks ensures that the perovskite catalyst exclusively contains trivalent cobalt. $\text{La}3\text{d}$ shows two regions with two peaks each one, corresponding to $\text{La}3\text{d}_{5/2}$ (834.5 and 837.6 eV) and $\text{La}3\text{d}_{3/2}$ (851.2 and 854.8 eV). These values again ensure the presence of La(III) as it is observed in La_2O_3 [29]. XPS spectrum of $\text{O}1\text{s}$ level presents two high features at 531.2 and 528.7 eV. The lower value could be attributed to oxide state, O^{2-} , characteristic of perovskite oxide network; while the higher value mainly represents the existence of hydroxyl groups in the surface, or adsorbed oxygen arising from atmospheric exposure [29,35,36]. The atomic superficial percentages, after a Shirley type background subtraction were 15.05, 11.48 and 57.25 for La, Co and O, respectively. These values differ from atomic ratios reported by EDX and XRF techniques, leading to a higher O proportion. Since XPS is a superficial analysis, the reason of this behavior may be originated from the presence of hydroxylated groups onto the surface of the solid.

In order to assess the effect of temperature during the process of calcination, a sample dried at 105–110 °C before being annealing was characterized by means of Thermal Gravimetry, Differential Temperature Analysis and released gases Mass Spectrometry (TG-DTA-MS) and X-ray Diffraction (XRD). TG spectrum (Fig. 9) shows a weak and continuous weigh loss up to 120 °C due to water desorption and condensation of hydroxyl groups, being accompanied with a slightly exothermic peak at 157 °C. Firstly, from this temperature until ~320 °C, H_2O and CO_2 are continuously released. In a second stage, at 347 °C a maximum of CO_2 release and an exothermic DTA peak are appreciated. This fact is the result of organic species burning and solid-state reaction. At this temperature a change in TG rate is also observed. DTA peak keeps increasing until 480 °C, sharply decreasing at 500 °C, when combustion is supposed to be finished. After 500 °C, no significant changes in TG, DTA and released gases are appreciated. A final 71.3% of mass loss is observed. In this loss, 15.76% is associated to H_2O and 79.9% corresponds to CO_2 . A final 4.35% is due to minor gases which accompany the two CO_2 release steps. H_2 is appreciated in the second and most important release

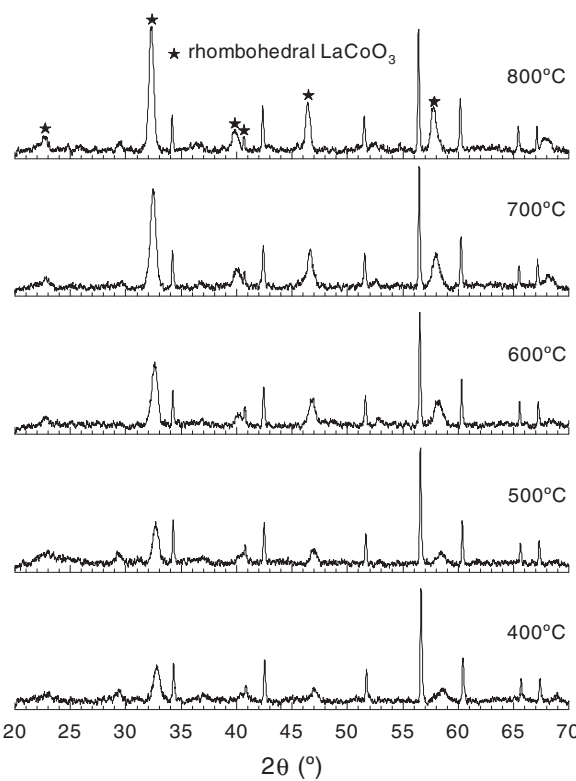


Fig. 10. XRD patterns of LaCoO_3 precursor during calcination process.

of CO_2 . Mass 58 may be identified as an acetone derivate. The simultaneous release of mass 15 may correspond to methyl fragments. A very low intensity mass 36 is observed, which might be tentatively identified as a sulfur derivative.

XRD in a thermal untreated sample was carried out, in order to assess the effect of temperature in LaCoO_3 structure formation. Results are depicted in Fig. 10. During the calcination process rhombohedral LaCoO_3 perovskite-type symmetry is formed [29,30,34]. At low temperatures, e.g. 600 °C, a semiquantitative analysis outlines $\text{Co}(\text{OH})_2$ (hexagonal, 18.9%), Co_3O_4 (cubic, 9.6%), $\text{La}_2\text{O}_2\text{CO}_3$ (hexagonal, 11.3%), La_2O_3 (cubic, 2.3%), CoCO_3 (rhombohedral, 48.5%) and $\text{La}(\text{OH})_3$ (hexagonal, 9.4%) as the main species. Hydroxides and carbonated precursors are likely to be responsible for LaCoO_3 formation. As temperature increases, the intensity of the starting patterns gradually diminishes and the peaks of perovskite structure increase. Thus, at 800 °C the sample is composed mainly by LaCoO_3 (rhombohedral, 83.6%), and small amounts of La_2O_3 (hexagonal, 8.5%) and Co_3O_4 (cubic, 7.9%).

4. Conclusions

LaCoO_3 shows a high activity with unappreciated cobalt leaching at neutral or basic pH. While acidic conditions accelerate the process due to homogeneous contribution from cobalt leaching, basic pH also worsens MPS decomposition rate. Furthermore, catalyst stability was analyzed by means of consecutive recycling uses and no significant loss in removal rate activity was experienced. pH and stability highly concern the nature of water which is suitable to be considered for this technology. Herbicides as micropollutants are frequently screened in natural water resources, whose pH is usually around circumneutral conditions. Thus, natural waters with a low content of organic matter and neutral or slightly basic pH are recommended.

Oxone® concentration up to 10^{-4} M led to a complete elimination of herbicides, being tritosulfuron the most recalcitrant

compound. Experiments in the presence of *tert*-butyl alcohol indicate that MPS decomposes onto the perovskite surface. The technology seems to be suitable for removing organic pollutants even at mg L^{-1} concentrations.

Solid LaCoO_3 settles down easily which is an advantage if compared to other catalysts. Moreover, since load does not significantly improve reaction rate, a low concentration would be enough for activating MPS decomposition, facilitating its recovering from the solution.

SEM and TEM techniques reveal the formation of nanosized particles, mainly spherical shaped. A poor $15.20 \text{ m}^2 \text{ g}^{-1}$ BET area was found and LaCoO_3 perovskite presence was remarked by diverse techniques such as X-ray Fluorescence (La:Co atomic ratio of 1:1), X-ray Photoelectron Spectroscopy (surface Co(III) and La(III)), and X-ray Diffraction (rhombohedral LaCoO_3 phase). TG-DTA-MS and XRD corroborated the formation of perovskite at temperatures higher than 700 °C.

Future work should be focused on assessing the possibilities of this perovskite catalyst in combination with some photocatalysts. Adding radiation might enhance MPS decomposition and radicals' production.

Acknowledgements

Authors thank economic support received from Gobierno de Extremadura and CICYT of Spain through Projects GRU10012 and CTQ2012-35789-C02-01, respectively. Mr. Rafael Rodríguez Solís also thanks Gobierno de Extremadura, Consejería de Empleo, Empresa e Innovación, and FSE Funds for his Ph.D. grant (PD12058). Catalyst characterization was provided by Facility of Analysis and Characterization of Solids and Surfaces of SAIUEx (financed by UEX, Junta de Extremadura, MICINN, FEDER and FSE).

Appendix A. Supplementary data

Supplementary data associated with this article can be found, in the online version, at <http://dx.doi.org/10.1016/j.apcatb.2016.06.058>.

References

- [1] T. Reemtsma, L. Alder, U. Banasiak, Water Res. 47 (2013) 5535–5545.
- [2] C. Moschet, I. Wittmer, J. Simovic, M. Junghans, A. Piazzoli, H. Singer, C. Stamm, C. Leu, J. Hollender, Environ. Sci. Technol. 48 (2014) 5423–5432.
- [3] Z. Vryzas, G. Vassiliou, C. Alexoudis, E. Papadopoulou-Mourkidou, Water Res. 43 (2009) 1–10.
- [4] E. Herrero-Hernández, M.S. Andrades, A. Álvarez-Martín, E. Pose-Juan, M.S. Rodríguez-Cruz, M.J. Sánchez-Martín, J. Hydrol. 486 (2010) 234–245.
- [5] E. Silva, M.A. Daam, M.J. Cerejeira, Chemosphere 135 (2015) 394–402.
- [6] P. Hu, M. Long, Appl. Catal. B: Environ. 181 (2016) 103–117.
- [7] Y.Q. Gao, N.Y. Gaoa, Y. Dengb, D.Q. Yina, Y.S. Zhangc, W.L. Rongc, S.D. Zhouc, Desalination Water Treat. 56 (2015) 2225–2233.
- [8] S. Yang, P. Wang, X. Yang, L. Shan, W. Zhang, X. Shao, R. Niu, J. Hazard. Mater. 179 (2010) 552–558.
- [9] G.P. Anipsitakis, D.D. Dionysiou, Environ. Sci. Technol. 38 (2004) 3705–3712.
- [10] D.G. Barceloux, Clin. Toxicol. 37 (1999) 201–216.
- [11] G.P. Anipsitakis, E. Stathatos, D.D. Dionysiou, J. Phys. Chem. B 109 (2005) 13052–13055.
- [12] Y. Ren, L. Lin, J. Ma, J. Yang, J. Feng, Z. Fan, Appl. Catal. B: Environ. 165 (2015) 572–578.
- [13] O.P. Tarana, A.B. Ayusheev, O.L. Ogorodnikova, I.P. Prosvirin, L.Z. Isupova, V.N. Parmon, Appl. Catal. B: Environ. 180 (2016) 86–93.
- [14] M. Carbajo, F.J. Beltrán, O. Gimeno, B. Acedo, F.J. Rivas, Appl. Catal. B: Environ. 74 (2007) 203–210.
- [15] F.J. Rivas, M. Carbajo, F. Beltrán, O. Gimeno, J. Frades, Appl. Catal. B: Environ. 155 (2008) 407–414.
- [16] J.L. Sotelo, G. Ovejero, F. Martínez, J.A. Melero, A. Milieni, Appl. Catal. B: Environ. 47 (2004) 281–294.
- [17] J.S. Noh, J.A. Schwarz, Carbon 28 (1990) 675–682.
- [18] M. Fukushima, K. Tatsumi, Environ. Sci. Technol. 39 (2005) 9337–9342.
- [19] J. Ghasemi, Sh. Ahmadi, K. Torkestani, Anal. Chim. Acta 487 (2003) 181–188.
- [20] P. Shukla, H. Sun, S. Wang, H.M. Ang, M.O. Tadé, Sep. Purif. Technol. 77 (2011) 230–236.

[21] J. Rivas, O. Gimeno, M. Carbajo, T. Borralho, *World Acad. Sci. Eng. Technol.* 57 (2009) 218–222.

[22] O. Gimeno, J. Rivas, M. Carbajo, T. Borralho, *World Acad. Sci. Eng. Technol.* 57 (2009) 223–226.

[23] B.S. Wolfenden, R.L. Willson, *J. Chem. Soc. Perkin. Trans. II* (1982) 805–812.

[24] H. Eibenberger, S. Steenken, P. O'Neill, D. Schulte-Frohlinde, *J. Phys. Chem.* 82 (1978) 749–750.

[25] G.V. Buxton, C.L. Greenstock, W.P. Helman, A.B. Ross, *J. Phys. Chem. Ref. Data* 17 (1988) 513–886.

[26] G.V. Buxton, A.J. Elliot, *Int. J. Radiat. Appl. Instrum. C. Radiat. Phys. Chem.* 27 (1986) 241–243.

[27] L. Dogliotti, E. Hayon, *J. Phys. Chem.* 71 (1967) 2511–2516.

[28] P. Ulanski, C. Sonntag, *J. Chem. Soc.* 2 (1999) 165–168.

[29] M.M. Natile, E. Ugel, C. Maccato, A. Gisenti, *Appl. Catal. B: Environ.* 72 (2007) 351–362.

[30] L. Predoana, B. Malic, M. Kosec, M. Carata, M. Calderaru, M. Zaharescu, *J. Eur. Ceram. Soc.* 27 (2007) 4407–4411.

[31] G. Xiong, Z.L. Zhi, X. Yang, L. Lu, X. Wan, *J. Mater. Sci. Lett.* 16 (1997) 1064–1068.

[32] Y. Wang, X. Yang, L. Lu, X. Wang, *Termochim. Acta* 443 (2006) 225–230.

[33] Y. Yamada, K. Yano, D. Honga, S. Fukuzumi, *Phys. Chem. Chem. Phys.* 14 (2012) 5753–5760, <http://dx.doi.org/10.1039/C2CP00022A>.

[34] Z. Yang, Y. Huang, B. Dong, H.L. Li, S.Q. Shi, *Appl. Phys. A* 84 (2006) 117–122.

[35] Y. Wang, J. Ren, Y. Wang, F. Zhang, X. Liu, Y. Guo, G. Lu, *J. Phys. Chem. C* 112 (2008) 15293–15298.

[36] L. Armelao, G. Bandoli, D. Barreca, M. Bettinelli, G. Bottaro, A. Caneschi, *Surf. Interface Anal.* 34 (2002) 112–115.